



## NRC Publications Archive Archives des publications du CNRC

### **Probabilistic analysis of local ice loads on a lifeboat measured in full-scale field trials**

Rahman, Md Samsur; Taylor, Rocky S.; Kennedy, Allison; Ré, António Simões; Veitch, Brian

This publication could be one of several versions: author's original, accepted manuscript or the publisher's version. / La version de cette publication peut être l'une des suivantes : la version prépublication de l'auteur, la version acceptée du manuscrit ou la version de l'éditeur.

For the publisher's version, please access the DOI link below. / Pour consulter la version de l'éditeur, utilisez le lien DOI ci-dessous.

#### **Publisher's version / Version de l'éditeur:**

<https://doi.org/10.1115/1.4030184>

*Journal of Offshore Mechanics and Arctic Engineering*, 137, 4, 2015-08-01

#### **NRC Publications Record / Notice d'Archives des publications de CNRC:**

<https://nrc-publications.canada.ca/eng/view/object/?id=af839bbf-9248-4c2f-bef9-f8a3da466a23>

<https://publications-cnrc.canada.ca/fra/voir/objet/?id=af839bbf-9248-4c2f-bef9-f8a3da466a23>

Access and use of this website and the material on it are subject to the Terms and Conditions set forth at

<https://nrc-publications.canada.ca/eng/copyright>

READ THESE TERMS AND CONDITIONS CAREFULLY BEFORE USING THIS WEBSITE.

L'accès à ce site Web et l'utilisation de son contenu sont assujettis aux conditions présentées dans le site

<https://publications-cnrc.canada.ca/fra/droits>

LISEZ CES CONDITIONS ATTENTIVEMENT AVANT D'UTILISER CE SITE WEB.

**Questions?** Contact the NRC Publications Archive team at

PublicationsArchive-ArchivesPublications@nrc-cnrc.gc.ca. If you wish to email the authors directly, please see the first page of the publication for their contact information.

**Vous avez des questions?** Nous pouvons vous aider. Pour communiquer directement avec un auteur, consultez la première page de la revue dans laquelle son article a été publié afin de trouver ses coordonnées. Si vous n'arrivez pas à les repérer, communiquez avec nous à PublicationsArchive-ArchivesPublications@nrc-cnrc.gc.ca.



## Md Samsur Rahman<sup>1</sup>

Faculty of Engineering and Applied Science,  
Memorial University of Newfoundland,  
S. J. Carew Building,  
Arctic Avenue,  
St. John's, NL A1B 3X5, Canada  
e-mail: msr303@mun.ca

## Rocky S. Taylor

Centre for Arctic Resource Development, C-CORE,  
Memorial University of Newfoundland,  
Bartlett Building,  
Morrissey Road,  
St. John's, NL A1B 3X5, Canada  
e-mail: rocky.taylor@card-arctic.ca

## Allison Kennedy

National Research Council of Canada,  
1 Arctic Avenue,  
P.O. Box 12093,  
St. John's, NL A1B 3T5, Canada  
e-mail: Allison.Kennedy@nrc-cnrc.gc.ca

## António Simões Ré

National Research Council of Canada,  
1 Arctic Avenue,  
P.O. Box 12093,  
St. John's, NL A1B 3T5, Canada  
e-mail: Antonio.SimoesRe@nrc-cnrc.gc.ca

## Brian Veitch

Faculty of Engineering and Applied Science,  
Memorial University of Newfoundland,  
S. J. Carew Building,  
Arctic Avenue,  
St. John's, NL A1B 3X5, Canada

# Probabilistic Analysis of Local Ice Loads on a Lifeboat Measured in Full-Scale Field Trials

*This paper presents an analysis of local ice loads measured during full-scale field trials conducted in 2014 with a totally enclosed motor propelled survival craft (TEMPSC) in controlled pack ice conditions. These data were collected as part of an ongoing research program that aims to identify the limitations of conventional TEMPSC operating in sea ice environments and to provide insight as to how these limitations might be extended. During the 2014 trials, local ice loads were measured at two locations on the TEMPSC's bow area. These loads were the most severe measured to date and corresponded to an average ice floe mass that was approximately 1.25 times the mass of the fully loaded TEMPSC. The event-maximum method of local ice pressure analysis was used to analyze these field data to improve understanding of the nature of ice loads for such interactions and to evaluate the suitability of this approach for design load estimation for TEMPSCs (i.e., lifeboats) in ice. The event-maximum method was adapted for the present application, so as to link exceedance probabilities with design load levels for a given scenario. Comparison of the 2014 results with a previous analysis of 2013 field trials data supports earlier conclusions that these interactions are highly influenced by kinetic energy, since more massive ice floes are observed to impart significantly higher loads on the lifeboats. Illustrative examples examining the influence of ice concentration and sail-away distance have also been provided. The work establishes links between extreme loads and the exposure of the lifeboat to ice for different operating conditions. Based on this work it is concluded that the event-maximum method provides a promising approach for establishing risk-based design criteria for lifeboats if field data are available which adequately represent ice conditions encountered during the design life of the lifeboat.*

[DOI: 10.1115/1.4030184]

## Introduction

Lifeboats are the most common type of survival craft and in an emergency may have to be used in sea ice conditions. These small craft are usually made from composite materials (glass reinforced plastics-(GRP)) and are designed for temperate regions that do not contain ice. Although their fiberglass hulls are adequate in open water conditions, there is a lack of design and operating standards that consider ice conditions [1]. In addition, there is a lack of information relating to the durability of marine composite hulls subject to various ice loads while transiting through prevailing ice conditions under power. Compared to the high strength steel typically used in larger ice-going vessels, the composite materials used in lifeboats are very flexible, which means that the ice-structure interaction between the composite structure and ice is markedly different than what is seen with stiff steel structures.

The use of lifeboats in more severe ice conditions is anticipated to increase in the coming years, as the offshore petroleum and minerals industries explore for and develop resources in northern frontiers. Conventional lifeboats, which are fitted on vessels and offshore petroleum installations as a means to evacuate personnel during hazardous situations, may not have the required

capabilities to operate in some ice conditions because of their low hull strength and limited navigational capabilities [2]. Regulations and standards [3] define the broad performance goals of escape, evacuation, and rescue systems, but do not offer any detailed design guidance related to the structural strength of lifeboat hulls during ice loading.

This paper focuses on the analysis of local ice load data, measured during full-scale lifeboat trials, using the "event-maximum" method [4]. This method was originally developed to analyze local ice loads measured on icebreakers based on probabilistic approaches. Later, an update to this method was proposed by Taylor et al. [5]. The revised method was adapted for analyzing the peak loads measured on the lifeboat during field trials for various ice-interaction scenarios that help to inform design methodology for evacuation craft operating in ice covered waters.

## Field Test Details

The 2014 field tests were completed in an ice covered lake using an instrumented, full-scale, TEMPSC. Details of the particulars of the ice field, full-scale TEMPSC, and instrumentation are provided below in the "Ice Field and Weather" section.

**Ice Field and Weather.** Field trials with an instrumented TEMPSC were carried out in March 2014 in a fresh water lake. The trials site consisted of a pool cut in the surrounding level ice. The pool was approximately 80 m long and 35 m wide. The ice

<sup>1</sup>Corresponding author.

Contributed by the Ocean, Offshore, and Arctic Engineering Division of ASME for publication in the JOURNAL OF OFFSHORE MECHANICS AND ARCTIC ENGINEERING. Manuscript received November 26, 2014; final manuscript received March 13, 2015; published online May 20, 2015. Assoc. Editor: Søren Ehlers.



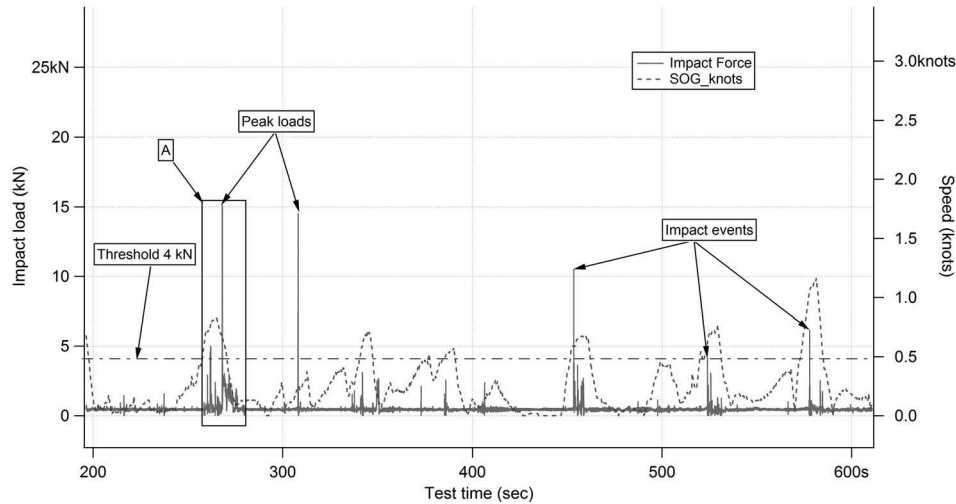


Fig. 2 Impact loads and speed of the same test

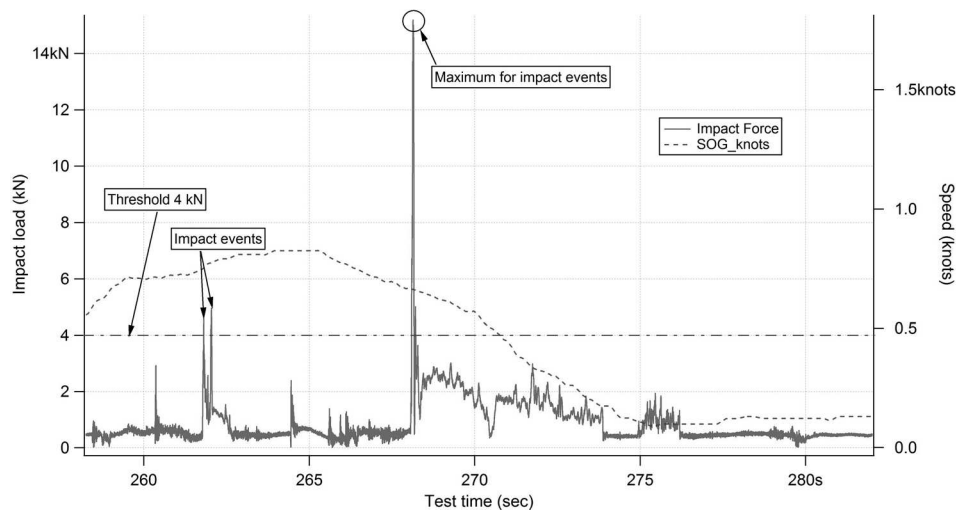


Fig. 3 Expanded load-time traces (section marked as A in Fig. 4)

### Distributions of Peak Ice Loads During Transiting

*Ice Load Distributions for Stem (2013 Data).* During each test, the TEMPSC progressed through a defined ice concentration and made a series of impacts with ice. The vessel's speed was variable, largely dependent on how it was operated by the coxswain. The overall distribution of 2013 stem load data for all tests is shown in Fig. 4.

Histograms for the high, medium, and low ice concentration cases are shown in Figs. 5–7, respectively. The frequency of low magnitude impact loads is high and decreases exponentially with increasing load. Impact loads on the stem are well fitted with a Weibull distribution in each category. More than 50% of all stem load events are lower than 8 kN. The largest load values on the horizontal coordinate of each histogram decrease slightly with decreasing ice concentration. The maximum ice load measured on the bow visor was 63.3 kN at high ice concentration, 57.4 kN at medium ice concentration, and 51.5 kN at low ice concentration level.

*Ice Load Distributions for Bow Shoulder (2013 Data).* Figures 8–11 illustrate the 2013 bow shoulder load histograms for all tests, high, medium, and low ice concentration cases, respectively. Again, the Weibull distribution provides a reasonable fit for all ice concentration categories. The maximum range of measured ice loads is significantly lower on the bow shoulder area than on the

stem. The maximum load measured on the bow shoulder was 34.3 kN during a test in a medium ice concentration level.

*Ice Load Distributions for Stem (2014 Data).* The overall distribution of 2014 stem load data for all tests is shown in Fig. 12. In the lower range, this distribution is generally consistent with the 2013 stem loads distribution as 43% of measured loads were below 8 kN during the 2014 field trials. The maximum range of impact loads is higher in the 2014 tests as is clearly seen from the histogram. Several loads measured during the 2014 tests had magnitudes higher than 63.3 kN (the highest load measured in 2013 tests). The maximum 2014 load was 117.9 kN. Similar operating conditions as the 2013 field test were maintained during 2014 field tests, except the use of heavier ice blocks having higher average ice thickness. The lifeboat experienced higher magnitude impact loads while it was progressing through the ice floes of higher mass than the previous year's tests.

Histograms for the high, medium, and low ice concentration cases are shown in Figs. 13–15, respectively. The largest load values on the abscissa of each histogram decrease slightly with decreasing ice concentration, as was the case for the 2013 stem load data.

*Ice Load Distributions for Bow Shoulder (2014 Data).* Figures 16–19 illustrate the 2014 bow shoulder load histograms for all tests, high, medium, and low ice concentration cases, respectively. The

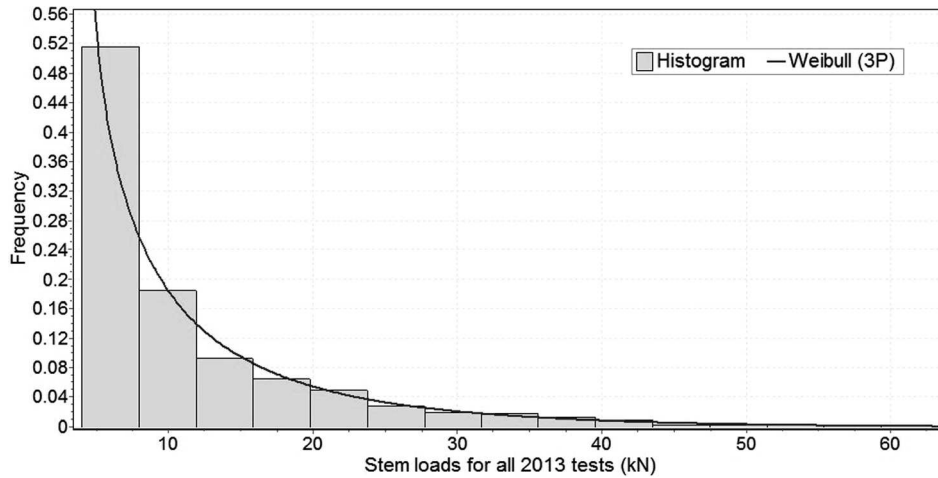


Fig. 4 Histogram of stem loads for all 2013 tests

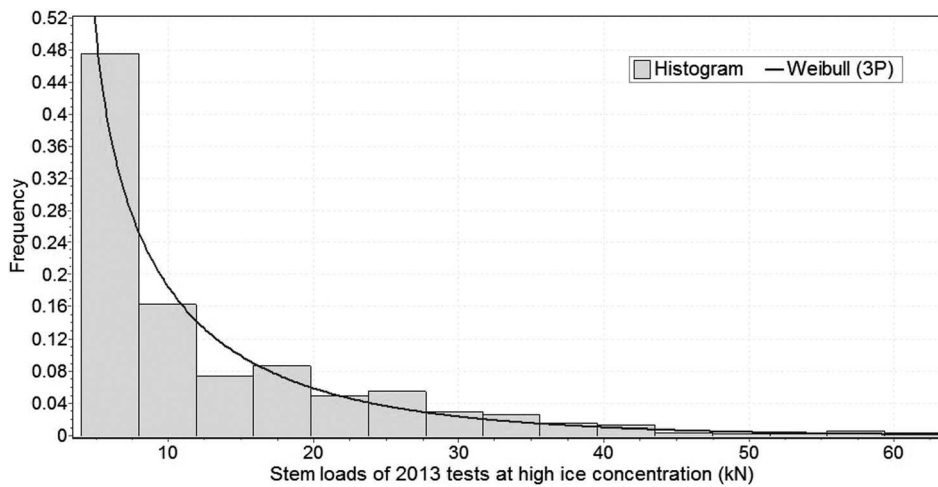


Fig. 5 Histogram of stem loads of 2013 tests at high ice concentration

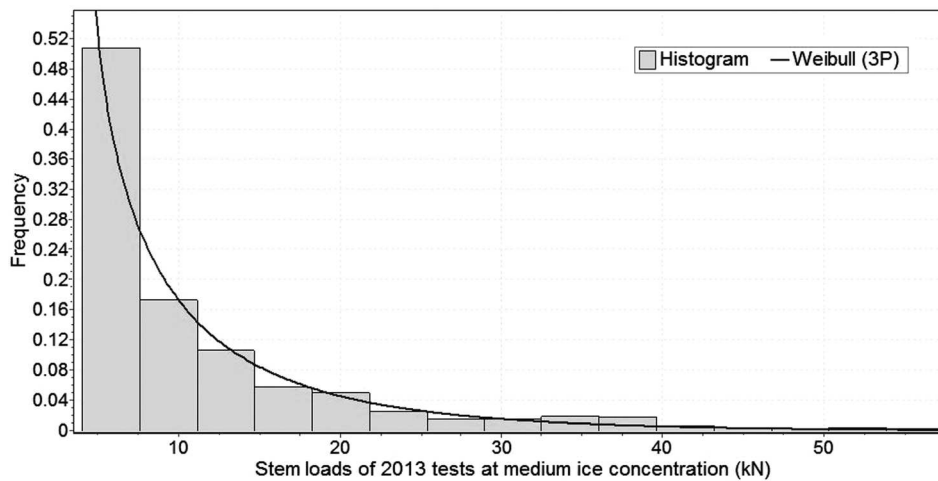


Fig. 6 Histogram of stem loads of 2013 tests at medium ice concentration

Weibull distributions are fitted for all ice concentration categories. The maximum range of measured ice loads is significantly lower on the bow shoulder area than on the stem. The maximum load measured on the bow shoulder was 62.7 kN, which is close to the highest load (63.3 kN) measured on the stem during 2013 field tests.

**Maximum Peak Loads During Straight-Line Impacts.** As discussed in Ref. [10], the maneuvering technique appears to have a strong effect on the impact load magnitude. While the maximum open water speed of the TEMPSC is approximately 6 kn, during the ice field transiting tests, the largest impact speed observed was

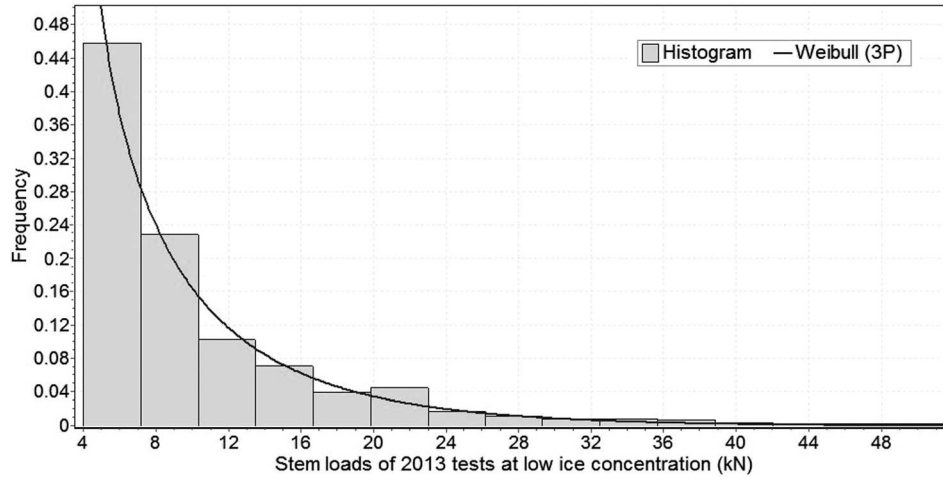


Fig. 7 Histogram of stem loads of 2013 tests at low ice concentration

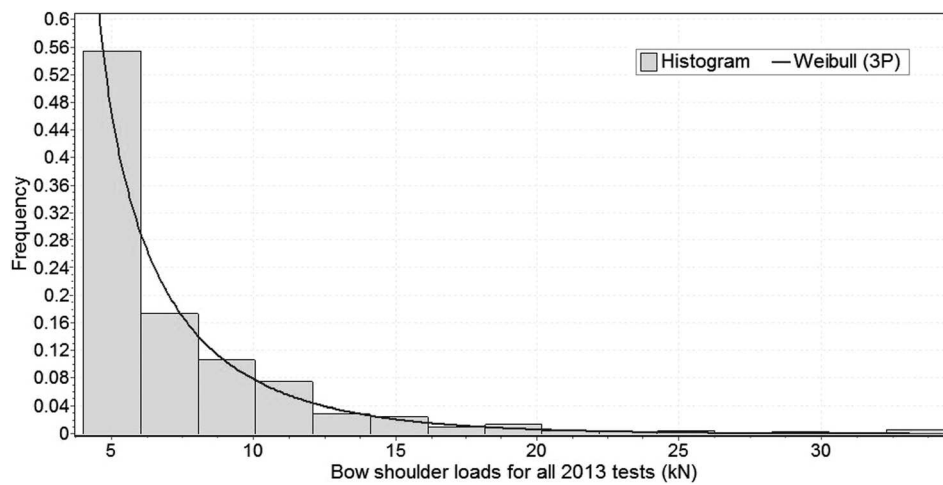


Fig. 8 Histogram of bow shoulder loads for all 2013 tests

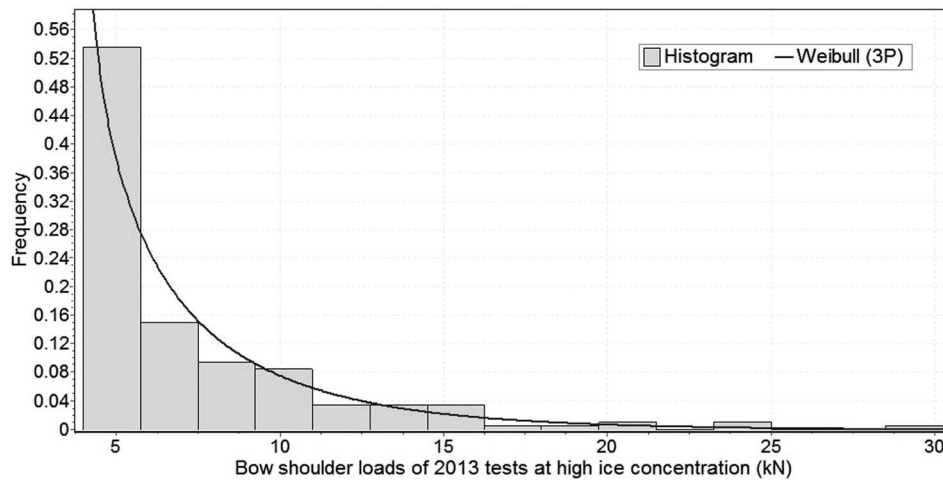


Fig. 9 Histogram of bow shoulder loads of 2013 tests at high ice concentration

approximately 3.5 kn. In general, impact speeds within the ice field were lower than 2 kn. A straight-line impact refers to a testing scenario where the vessel accelerates through a region of open water before directly impacting the ice floe, which leads to higher ice loads.

During the 2014 field trials, a subset of eight tests were conducted to measure the ice impact loads from events in which the TEMPSC transited at relatively high-speeds in comparison to speeds observed during ice field testing. These straight-line impact tests were carried out specifically with the goal of measuring extreme loads during

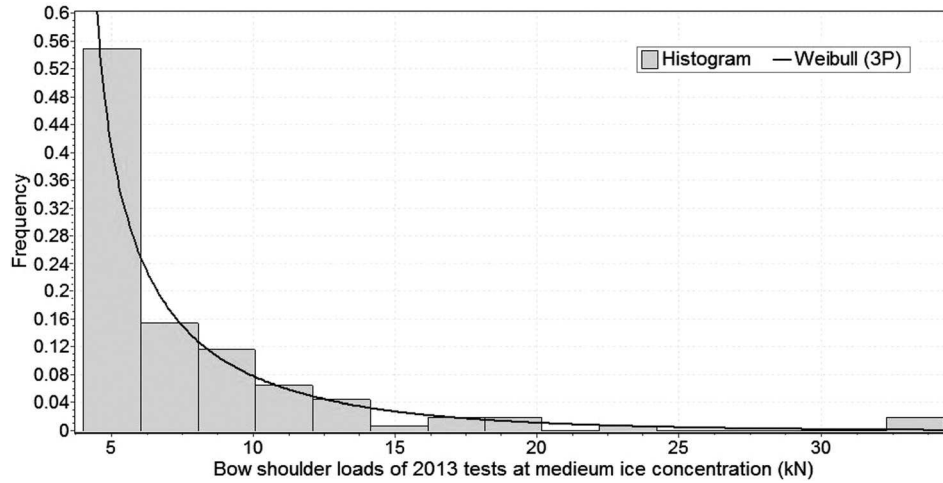


Fig. 10 Histogram of bow shoulder loads of 2013 tests at medium ice concentration

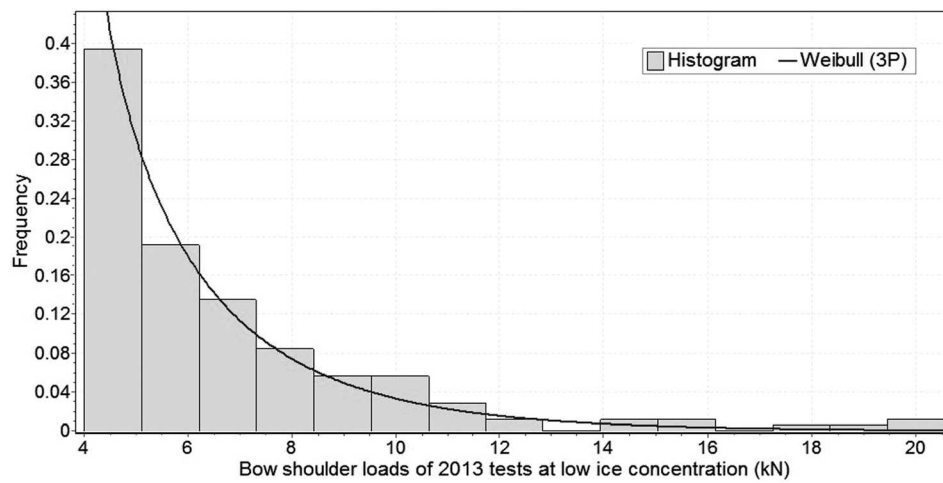


Fig. 11 Histogram of bow shoulder loads of 2013 tests at low ice concentration

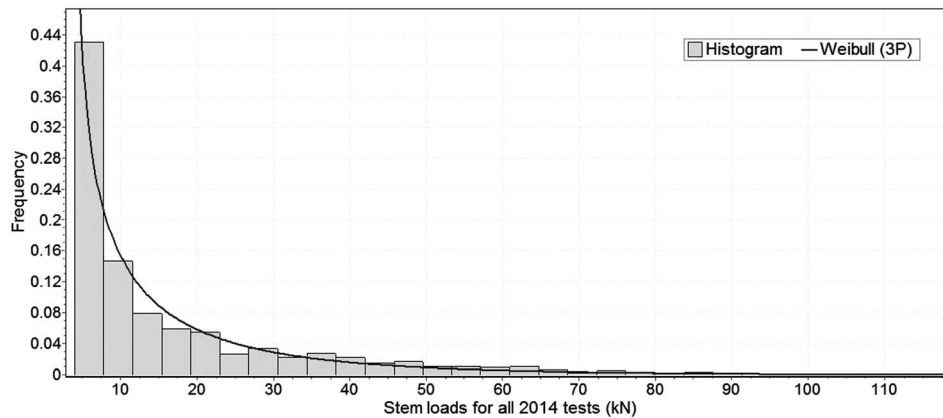


Fig. 12 Histogram of stem loads for all 2014 tests

individual impact events, rather than measuring loads that occurred while transiting under different conditions. In these tests, the TEMPSC navigated at set shaft speed values toward an individual ice floe and then impacted the ice floe at the stem.

In the present analysis, the data corresponding to these tests have been treated separately from the transiting data discussed in the Distribution of Peak Ice Loads During Transiting section.

Results from these eight tests were not included in the probabilistic analysis as this type of severe ramming condition was deemed to be unrepresentative of typical transiting operations used throughout the rest of the test program. However, it is recognized that in extreme circumstances, coxswains may possibly use such a technique when attempting to clear through the ice. The approach employed here is to use these straight-line impact data to perform

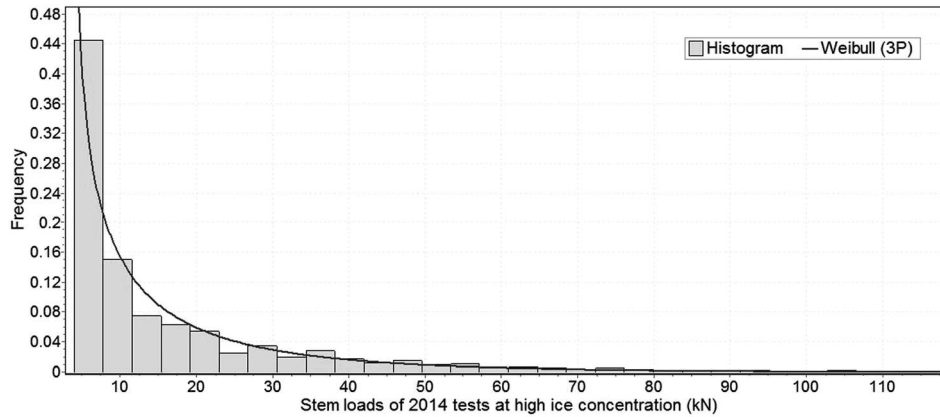


Fig. 13 Histogram of stem loads of 2014 tests at high ice concentration

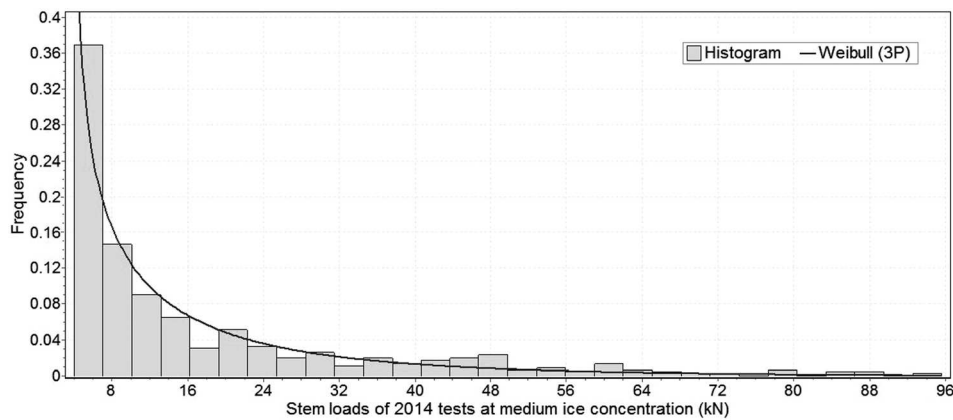


Fig. 14 Histogram of stem loads of 2014 tests at medium ice concentration

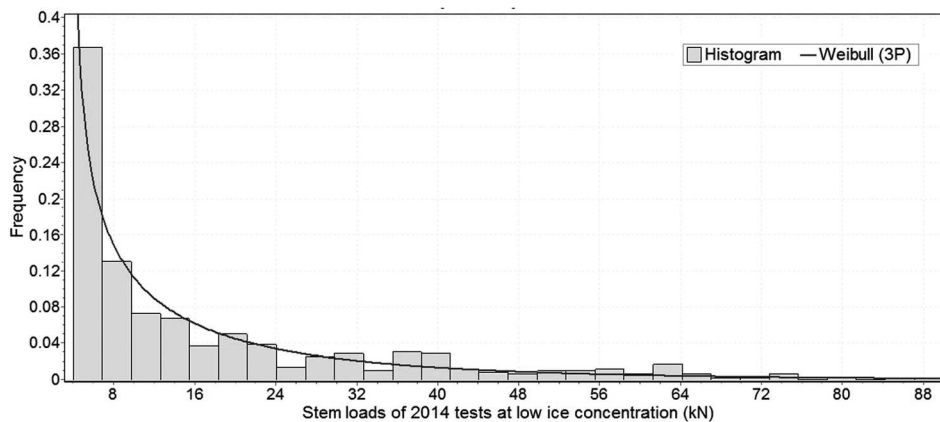


Fig. 15 Histogram of stem loads of 2014 tests at low ice concentration

an upper-bound check on design load estimates calculated with the 2014 ice transiting data using the event-maximum method. This is done to ensure the design satisfies the demands that would be placed on the lifeboat if the straight-line impact technique is employed.

Peak load data and other corresponding details associated with the straight-line impact tests are presented in Table 2. As observed in this table, the local ice impact loads at the stem ranged from 58 kN to 139 kN and the impact speed ranged from 1 kn to 6 kn. It is also observed that the instantaneous speed values corresponding to all maximum loading events are not consistently high. The load magnitudes from test 9 and test 32 were similar (94.9 kN versus

95.6 kN) but the corresponding TEMPSC speeds for each event are very different (0.4 kn versus 3.4 kn). In the case of test 9, the ice field contained a thin layer of level ice between the individual ice floes. This test was the first test performed during that day and a thin layer of solid ice had formed between the floes overnight. By comparison, the large stem load event that occurred during test 32 resulted from a direct impact with a free floating ice floe edge. The impact resulted in negligible damage to the ice piece but caused the ice floe to move away from the TEMPSC.

It is noted that the three smallest loads and the three lowest impact speeds correspond to low mass ice pieces ( $1.0 \times m_{TEMPSC}$ ). The impact loads were plotted against the impact speed to

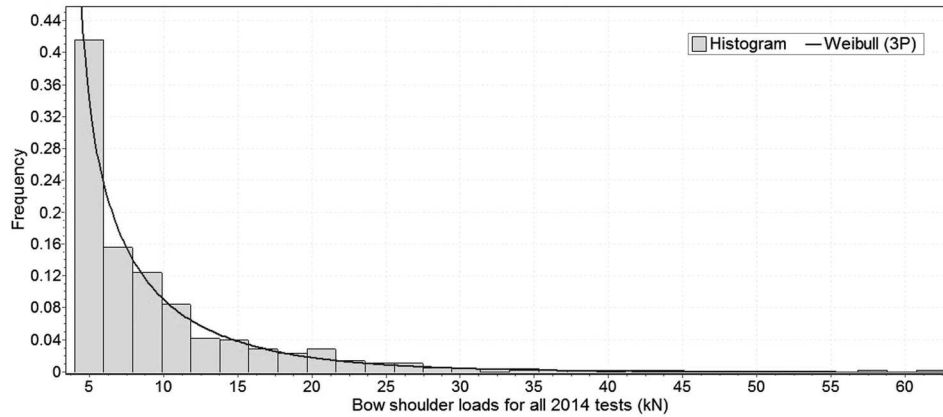


**Fig. 16 Histogram of bow shoulder loads for all 2014 tests**

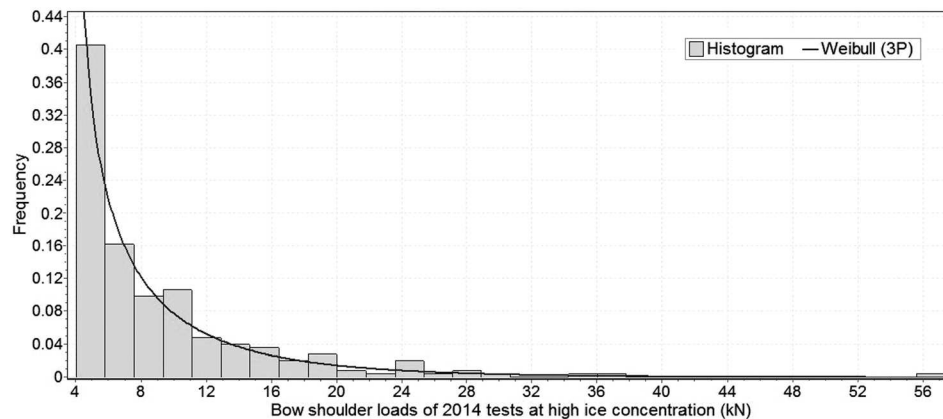


**Fig. 17 Histogram of bow shoulder loads of 2014 tests at high ice concentration**

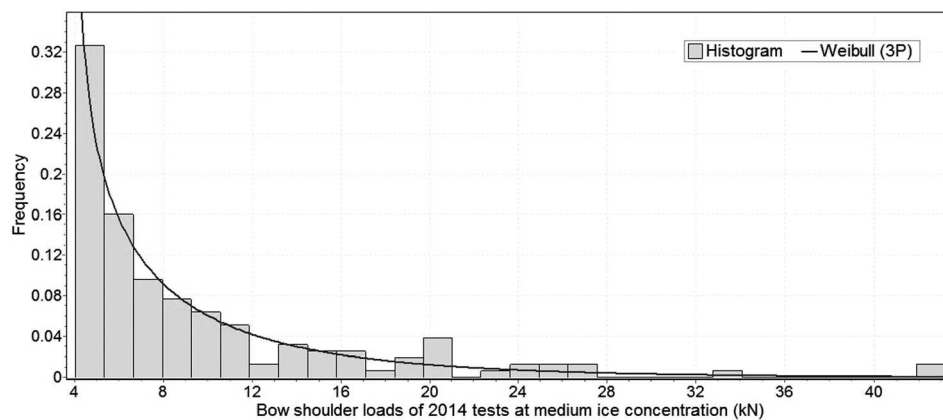


**Fig. 18 Histogram of bow shoulder loads of 2014 tests at medium ice concentration**

illustrate the correlation between the two parameters and highlight variations from this trend in the data (see Fig. 20). In general, the local ice load at the stem has a positive correlation with the impact speed. The correlation coefficient between stem load and TEMPSC speed, for the larger ice pieces, is approximately 0.88, although there are two data points that do not agree with this general observation. This is believed to be due to differences in the tests conditions associated with these two events. These points are indicated with superscripts in Fig. 20 and details that help to explain the differences are provided as comments in the figure.

The first of these noted points (marked with number 1 in Fig. 20) relates to an impact load of approximately 104 kN and an

impact speed of 1.5 kn. There was another high-speed impact test with the same ice floe mass and impact speed that resulted in a much lower impact force. During the test that resulted in the higher load, the ice floe was not fully independent: the aft edge of the ice floe was adjacent to ice floes within the ice field. In this case, when the TEMPSC hit the ice floe, it pushed the target ice floe as well as the adjacent floes. In all other individual ice floe impact tests, the ice floe was completely independent from the surrounding ice.

The second noted data point (marked with number 2 in Fig. 20) relates to the largest load observed during the straight-line impact tests, which corresponded to a force of 139.0 kN, a peak pressure

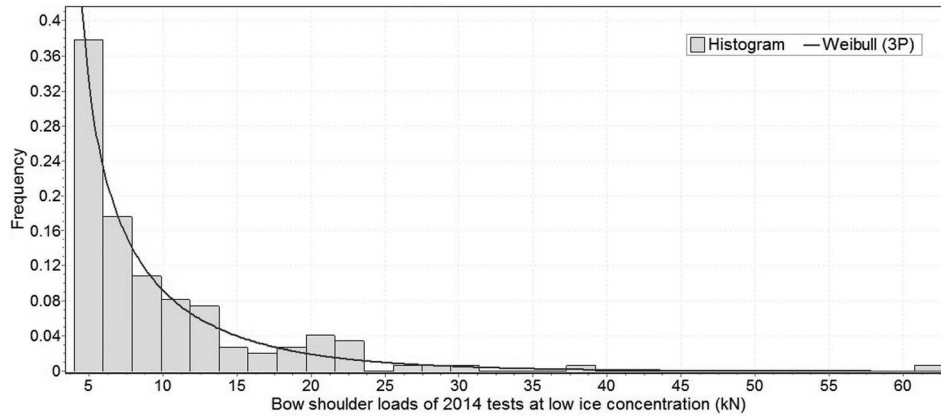


Fig. 19 Histogram of bow shoulder loads of 2014 tests at low ice concentration

Table 2 Largest stem and bow shoulder loads and corresponding TEMPSC speeds

Test #	Load location	Ice piece mass ( $\times m_{\text{TEMPSC}}$ )	TEMPSC speed (kn)	Maximum load (kN)	Maneuvering technique
9	Stem	1.25	0.4	94.9	Straight-line impact
32	Stem	1.25	3.4	95.6	Straight-line impact
11	Stem	1.25	0.8	102.9	Straight-line impact
8	Stem	1.25	1	105.1	Straight-line impact
6	Stem	1.25	2.3	117.9	Straight-line impact
18	Shoulder	1.25	0.7	57.4	Straight-line impact
45	Shoulder	2.25	2.1	62.7	Straight-line impact

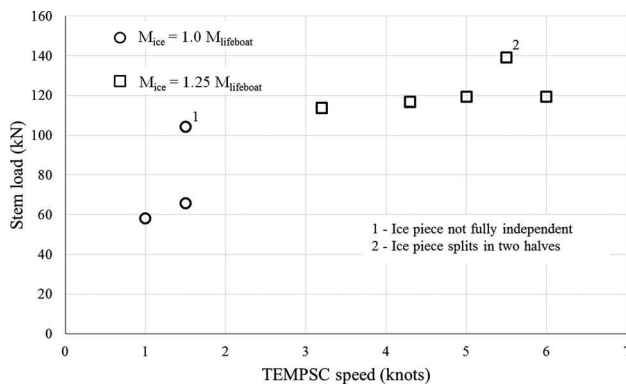


Fig. 20 Individual ice piece impacts stem loads

of 0.69 MPa over the panel area, and an impact speed of approximately 5.5 kn. The test at 5.5 kn resulted in the ice floe fracturing into two separate parts. This was the only test in the individual ice floe impact series that resulted in the floe being split into two halves and for all other tests, negligible damage to the ice floe was observed. The load associated with this test is significantly higher than the impact load measured during a similar test conducted at an impact speed of 6.0 kn. A possible implication of this result is that higher loads may have been experienced by the lifeboat if the ice floe did not fail (e.g., a thicker or stronger floe).

It is important to highlight here that during all of the straight-line impacts and other field experiments discussed in this paper, no damage to the lifeboat was observed. Similarly, no cumulative damage effects associated with fatigue were observed, and fatigue was not identified as being a concern for the loading scenarios considered.

**Local Ice Design Pressures for Transiting Conditions.** To model the extreme loads of interest in design for a lifeboat transiting through a broken ice field, the event-maximum method was

applied to the ice transiting data set (straight-line impact data points were not included here). According to the event-maximum method, which has been effectively applied for the analysis of local ice pressure data sets for other types of vessels and structures [3–5], the peak pressures calculated from the measured loads were ranked in descending order on a given area for high, medium, and low ice concentrations and plotted against the natural logarithm of the plotting position ( $P_e$ ). The Weibull plotting position was used for simplicity, given as  $[i/(j+1)]$ , where  $i$  is the rank of the individual data points from a set of  $j$  pressures. Based on the techniques presented in Refs. [4,5], a best-fit line was fitted to the tail (top 20% peak pressures) of each distribution, which was assumed to follow an exponential distribution, to give

$$F_x(x) = 1 - \exp(-(x - x_0)/\alpha) \quad (1)$$

where  $x_0$  and  $\alpha$  are constants for a given area, and  $x$  is a random quantity denoting pressure. The parameter  $\alpha$  is the inverse slope of the best-fit line, and  $x_0$  is the intercept of this line with the abscissa. Here, the parameter  $\alpha$  is a function of area, represented by the curve  $\alpha = Ca^D$ , where  $\alpha$  is the local area of interest, and  $C$  and  $D$  are constants that depend on the physical characteristics of ice, while the parameter  $x_0$  represents the exposure for a given design curve [4,5]. It is noted that the values of these parameters are determined so as to provide the best agreement between the model and the extreme load values in the tail of the probability distribution. As a consequence, it is possible that a nonphysical negative value of  $x_0$  could potentially result during an analysis. This does not mean that a negative pressure may occur, but rather is a merely reflection of the parameter values required in this method to best model the extreme loads. If one is interested in capturing the typical range of pressures encountered during operations, rather than the extremes for design, other approaches such as those used to generate Figs. 4–19 may be better suited (albeit at the cost of reduced model accuracy for extreme loads).

This analysis was completed for the loads that occurred at the TEMPSC stem and bow shoulder independently, resulting in two unique plots of local pressure. For this analysis, emphasis is on

the peak loads measured in a given ice concentration. The results of each assessment were compared to the results of a similar analysis conducted on data from previous 2013 field tests [11].

*Stem.* As this analysis is driven by an interest in design loads, the analyses are performed using the top 20% of loads measured at each ice concentration category, based on the event-maximum method of local pressure estimation. The local pressure curve representing the extreme values within the histograms is provided in Fig. 21. There does not appear to be a significant difference between the high, medium, and low ice concentration categories in the lower local ice pressure range. On the mid- to high-end of the local pressure range, the low, medium, and high concentration categories become more distinct and have uniquely defined trends. The  $\alpha$  and  $x_0$  values representative of the 2014 and 2013 data for each ice concentration category are summarized in Table 3.

The 2014 data for each ice category were compiled to develop a general local stem pressure curve representative of ice loads from all ice concentrations. This result was compared to a similar plot which was created for data resulting from a previous set of field trials conducted in 2013 [11]. During these previous field trials, the mass of a single ice floe was approximately equal to the mass of the fully loaded TEMPSC and thus smaller than the average ice floe mass in 2014 (by a ratio of 1:1.25). The general local stem pressure curves resulting from both 2014 data and 2013 data are provided in Fig. 22.

The local pressure curve for the stem based on 2014 data is distinctly different from that based on 2013 data. Both curves have strong trends with few outliers.

*Bow Shoulder.* The extreme values within the tail portions of each bow shoulder histogram were used to devise a local pressure curve representative of the bow shoulder (see Fig. 23). The local pressure values for the bow shoulder are much smaller than the pressure values for the stem (Fig. 21).

Consistent with the analysis process for the stem loads, the local pressure values for each ice concentration category were compiled to allow for development of a general local pressure curve. This general curve is representative of all ice loads

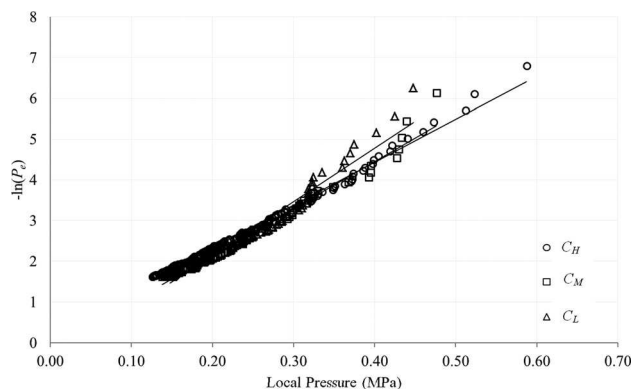


Fig. 21 Local pressure curve for impact events on the stem (2014)

Table 3 Parameters estimated from local pressure curve (2013 and 2014 stem loads)

Ice concentration	Stem loads 2013		Stem loads 2014	
	A (MPa)	$x_0$ (MPa)	$\alpha$ (MPa)	$x_0$ (MPa)
$C_H$	0.068	0.029	0.095	0.020
$C_M$	0.068	-0.002	0.087	-0.014
$C_L$	0.054	0.006	0.076	-0.008

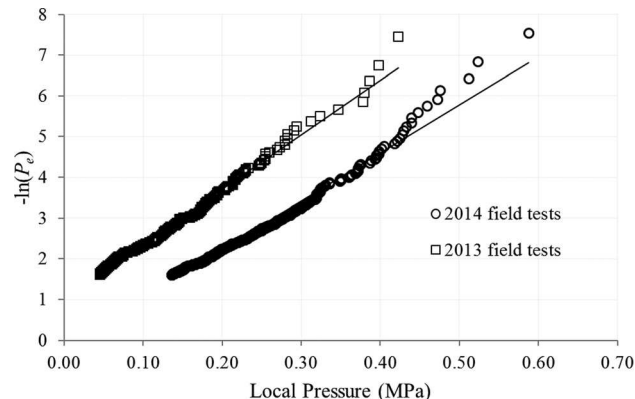


Fig. 22 Comparison of local pressure for impact events on the stem measured in 2013 and 2014 field tests

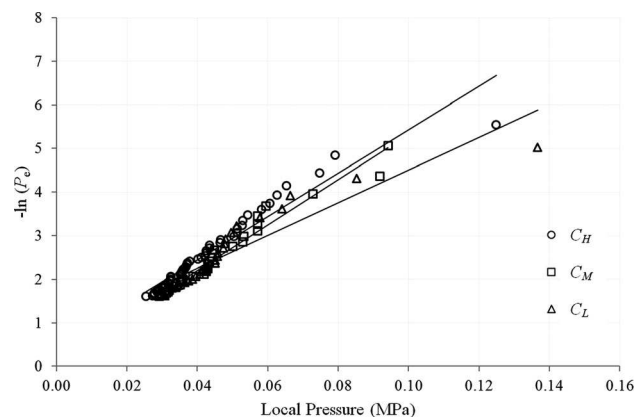


Fig. 23 Local pressure curve for impact events on the bow shoulder

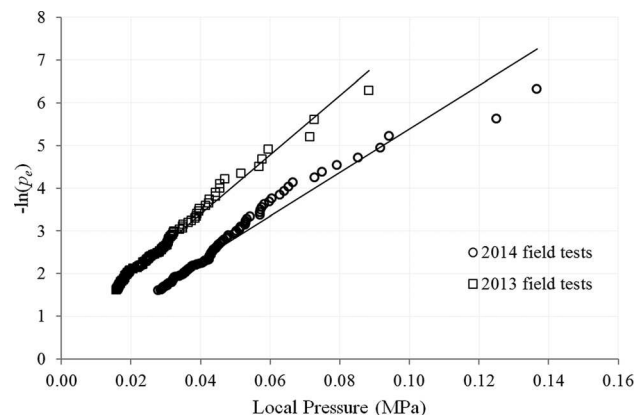


Fig. 24 Comparison of local pressure for impact events on the bow shoulder measured in 2013 and 2014 field tests

measured during 2014 field trials. This result was compared with a similar local pressure curve for the bow shoulder that was devised based on 2013 data. Both local pressure curves are provided in Fig. 24.

Similar to the 2013–2014 comparison of local stem pressure curves in Fig. 22, the local bow shoulder curve for 2014 was distinctly different from that resulting from 2013 data. The  $\alpha$  and  $x_0$  values representative of the bow shoulder for the 2014 and 2013 data are provided in Table 4. These values define the local bow shoulder pressure curves for each ice concentration category. The

**Table 4 Parameters estimated from local pressure curves (2013 and 2014 bow shoulder loads)**

Ice concentration	Bow shoulder loads 2013		Bow shoulder loads 2014	
	$\alpha$ (MPa)	$x_0$ (MPa)	$\alpha$ (MPa)	$x_0$ (MPa)
$C_H$	0.015	0.002	0.020	0.009
$C_M$	0.025	-0.018	0.019	0.002
$C_L$	0.011	0.005	0.027	0.020

**Table 5 Number of interaction events on the stem for different ice concentrations (2013 and 2014 tests)**

Number of events	2013 tests			2014 tests		
	$C_L$ (4–5)	$C_M$ (6–7)	$C_H$ (8–9)	$C_L$ (5)	$C_M$ (6–7)	$C_H$ (8–9)
$v$ (0.5 km)	125	225	325	375	575	775
$v$ (1.0 km)	250	450	650	750	1150	1550
$v$ (5.0 km)	1250	2250	3250	3750	5750	7750

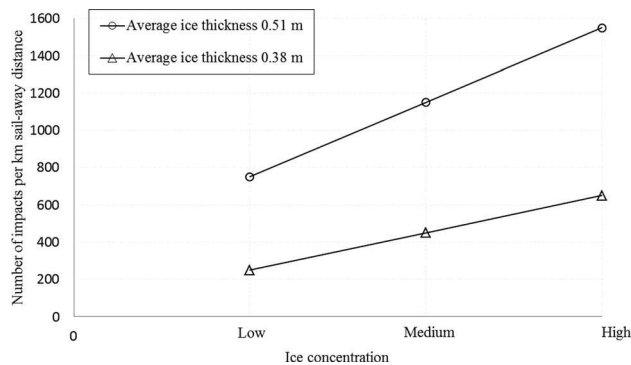


**Fig. 25 Comparison of expected number of ice impacts per kilometer sail-away distance at stem area in two different ice thicknesses**

$\alpha$  does not consistently increase or decrease with increasing ice concentration for the bow shoulder data. This is different from the alpha values determined from the stem load analysis.

**Exposure.** The exposure of the vessel is an important consideration in assessing the extreme load. One important aspect of exposure is the number of impact events that the vessel will encounter during a given time period. The number of impact events can depend on a variety of factors, such as the ice conditions (e.g., ice concentration and floe size), the required sail-away distance, and the threshold chosen for impact events. The effects of these factors are discussed below.

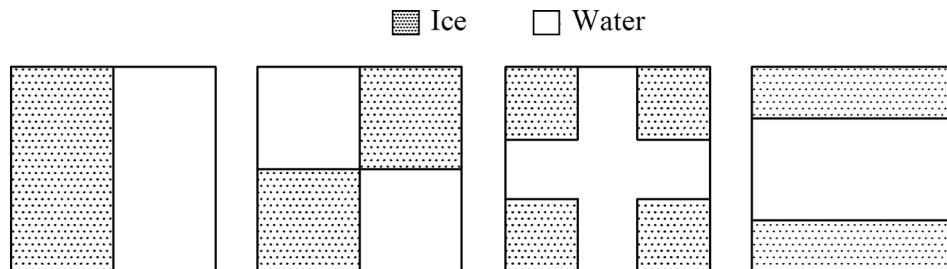


**Fig. 26 Idealizations of different ice floe configurations of five-tenth ice concentration**

**Ice Conditions.** An example is presented here to illustrate the effect of ice concentration and ice floe mass on the number of impacts. In defining example scenarios, the total sail-away distance was calculated by adding the sail-away distance values measured from each test in a given ice concentration category. The total number of interaction events for each ice concentration category was found by taking the sum of the total number of interaction events for each test in that given category. The average number of interaction events  $v$  per kilometer was then estimated by taking the total number of events and dividing by the total sail-away distance. This was calculated for low, medium, and high ice concentrations and the corresponding values are summarized in Table 5, for both 2013 and 2014 data. The actual distance (path length) transited may be larger than the sail-away distance, particularly for high ice concentrations where coxswains have to find their way through small leads in the ice.

A comparison of estimated number of impacts per kilometer of sail-away distance at the stem for two data sets, 2013 and 2014, is shown in Fig. 25. The level of exposure (number of impacts) increased with rising ice concentration, which indicates that the possibility of encountering ice impacts rises as the lifeboat passes through a denser pack ice region. In addition, the comparison of 2013–2014 data indicates that for the thicker ice conditions, a higher number of impact events with load levels exceeding the threshold occurred at each ice concentration level. The movement of the lifeboat through ice during 2014 trials was limited by the ice floes having a larger average mass than those in the 2013 trials, which resulted in a larger quantity of impacts and lower sail-away distances.

Navigation of small vessels through pack ice is sensitive to local variations of ice concentration. In applying this method, one must consider the local ice concentration as the individual floe sizes (mass) will have a big effect on resulting ice loads. Typically, ice concentration reflects an average areal distribution of ice in a region. As depicted in Fig. 26, different spatial configurations of ice will present very different operating environments. This also affects the number of impacts per kilometer of sail-away distance, which in turn influences design loads estimates.

**Sail-Away Distance.** It is important to consider how the exposure is defined in terms of sail-away distance and the ice concentration. To simplify the discussion, if we assume that each impact event corresponds to essentially a single floe–ship interaction, then we can illustrate, as in Fig. 27, the relationship for (a) constant exposure, different sail-away distances and (b) different exposures, constant sail-away distance in different ice concentration levels. In the first case, illustrated in Fig. 27(a), as the ice concentration increases, the sail-away distance required to be exposed to the same number of impacts decreases. The second case is illustrated in Fig. 27(b), which shows that if the vessel is transiting a fixed sail-away distance, we expect exposure to increase as ice concentration increases. In applying the techniques presented in the section Local Ice Design Pressure for Transiting Conditions, it is essential that a consistent basis is used to define exposure, which typically will correspond to the case of fixed sail-away distance, not a fixed number of impacts.

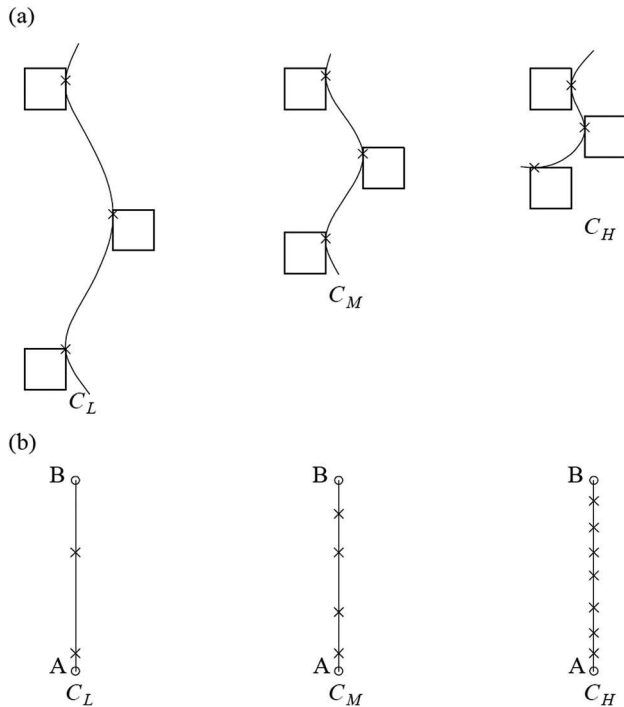


**Fig. 27 Effect of number of impacts and sail-away distance on exposure (a) constant exposure (constant number of impacts and different sail-away distance) and (b) different exposures (constant sail-away distance and different number of impacts)**

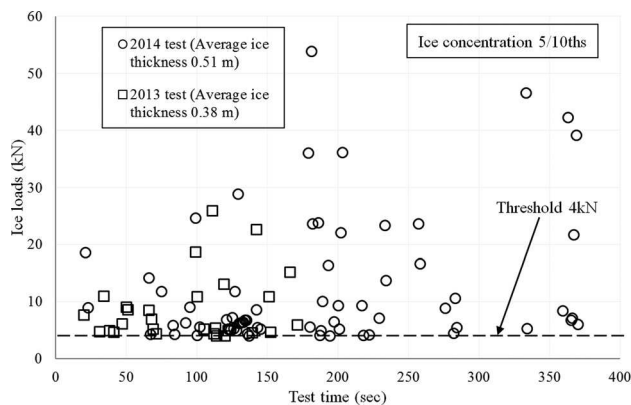


**Fig. 28 Threshold effect on the number of impacts in 2013 and 2014 test at five-tenth ice concentration**

*Threshold Effects.* For analyzing the data, a minimum ice load threshold of 4 kN was set for both 2013 and 2014 tests. In thicker ice (2014 tests), there were more events above the threshold as depicted in Table 5. For interactions with thicker ice, more impact events will result in loads that exceed the 4 kN threshold, which

results in larger numbers of events registering on the load panels. This threshold effect is illustrated in Fig. 28, in which the loads measured above the threshold are plotted against test time for two individual tests during 2013 and 2014 field trials. Both tests were performed in five-tenth ice concentration and in both, the TEMPSC traveled similar sail-away distances. The 2014 test involved a longer path length, longer test duration (due to the heavier ice floes), and a higher number of ice impacts when compared to the 2013 test. A significant number of the ice impacts that occurred during the 2014 test had a magnitude just above the threshold load value.

If a load (force) threshold is used in the analysis, as the ice thickness increases, the number of events exceeding the threshold will also increase. For example, the vessel may nominally come into contact (impact) 1000 ice features, but for the case of thin ice only 250 of those may register a load above 4 kN, whereas for thicker ice 650 events may register a load above the threshold.

**Illustrative Example.** To illustrate how the results may be used to estimate local design pressures for the stem, the event-maximum method is used to estimate the extreme pressure  $z_e$  using the following equation:

$$z_e = x_0 + \alpha \{-\ln[-\ln F_Z(z_e)] + \ln v + \ln r\} \quad (2)$$

where  $\alpha$  and  $x_0$  are constants,  $F_Z(z_e)$  is the exceedance probability,  $v$  is the expected number of events, and  $r$  is the expected proportion of impact loads on the given region. In this method,  $\alpha$  is generally taken as an area-dependent relationship that is determined from ship-ice impact data given by the expression

$$\alpha = Ca^D \quad (3)$$

where the coefficients  $C$  and  $D$  are empirical constants determined from ship-ice impact data [5]. For the present study, it is not possible to develop such an area-dependent relationship, since loads have only been collected for a single panel area at the stem/bow shoulder.

The values  $\alpha$  and  $x_0$  from Table 3 and the values for the expected number of events  $v$  given in Table 5 can be used to estimate the extreme pressures for the stem, summarized in Table 6. These extreme pressure estimates assume that the expected proportion of ice impacts on the stem,  $r$ , is 0.5 (e.g., 50% of the impacts occur on the stem panel, while all others occur on the sides or elsewhere on the vessel), and that  $F_Z(z_e)$  corresponds to a probability of exceedance of  $10^{-2}$ .

The extreme design pressures at the stem were calculated based on the 2013 and 2014 data sets separately. The design pressure values based on 2013 data and 2014 data are each illustrated in Fig. 29 for the 1.0 km transit distance case. Design pressure values are provided for each category of ice concentrations: low, medium, and high.

The design pressure guidance based on 2014 field results is distinctly higher than that from 2013 test results. This indicates that the design pressure should be higher for thicker (heavier floes) ice conditions. These design pressure values can be used to guide the design of ice capable evacuation craft and other GRP vessels that

**Table 6 Local design pressures at stem for example scenario**

Transit distance (km)	Stem local design pressures (MPa) for different ice concentrations and transit distances					
	2013 tests			2014 tests		
	$C_L$ (4–5)	$C_M$ (6–7)	$C_H$ (8–9)	$C_L$ (5)	$C_M$ (6–7)	$C_H$ (8–9)
0.5	0.48	0.63	0.69	0.74	0.88	1.02
1.0	0.52	0.68	0.74	0.79	0.94	1.09
5.0	0.60	0.79	0.84	0.91	1.08	1.24

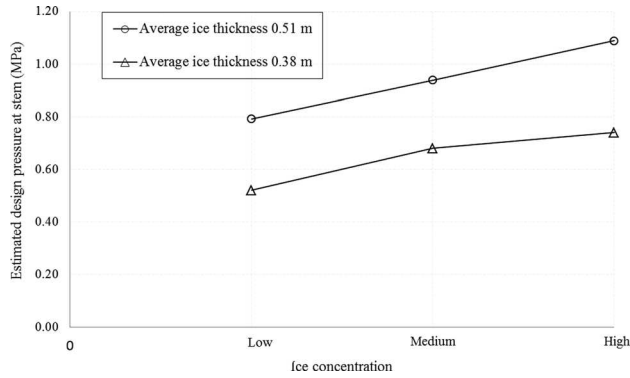


**Fig. 29 Comparison of estimated design pressure at stem for two different ice thicknesses**

operate in ice covered waters. It should be cautioned that more severe conditions, including thicker ice floes and floes with larger mass, will likely require a higher design pressure. This result reflects that when using empirical approaches as presented here, the parent distributions associated with a given set of measurements are reflective of that particular data set, which in turn is associated with a given combination of structural configurations and ice conditions, and not an underpinning physical law that can be universally applied. Consequently, one must exercise caution in applying those data to structure–ice combinations other than those embodied in the data.

### Discussion

The stem loads result in local pressure curves that are unique for high, medium, and low ice concentrations. These local pressure curves each represent different pressure levels and are defined with unique  $\alpha$  values that increase with increasing ice concentration (e.g., exposure). In contrast, the bow shoulder loads result in intermingled local pressure curves for the low, medium, and high ice concentrations. The  $\alpha$  values do not increase with increasing ice concentration. Therefore, a specific local pressure curve relevant to a certain range of ice concentrations may be used to guide the design pressure for the TEMPSC stem, whereas a generic local pressure curve may be more relevant for the bow shoulder.

The peak bow pressure measured for all transiting events during 2013 and 2014 field programs was about 0.42 MPa and 0.59 MPa, respectively. From Table 6, it is observed that the local design pressure for low ice concentrations and short transit distances corresponding to an exceedance probability of  $10^{-2}$  is 0.48 MPa and 0.74 MPa for 2013 and 2014 tests, respectively, which is greater than the measured peak bow pressure. It is important to note that the peak pressure value of 0.69 MPa corresponding to the maximum force of 139 kN from the 2014 straight-line impact data presented in Fig. 20 is also below the design value of 0.74 MPa based on the 2014 data. This result suggests that the proposed design method provides a conservative estimate of design pressure for the range of conditions considered in this study.

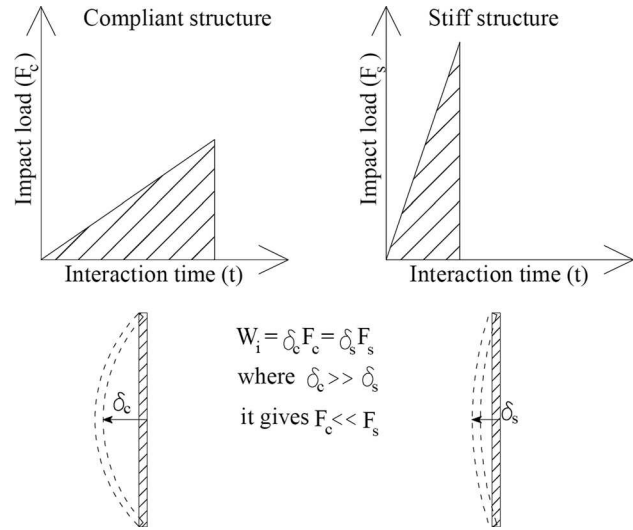


**Fig. 30 Impact load profile and deflection of compliant and stiff structure**

A comparison of the results of the probabilistic evaluation of 2014 data with 2013 data indicated a number of distinct differences. The level of exposure, or number of ice impacts above a given threshold at a given ice concentration level, was larger for an ice field with higher average ice piece mass. In addition, the magnitudes of peak ice loads measured in the higher ice piece mass cases (2014) were larger than those measured in an ice field with smaller average ice piece mass (2013). These two factors lead to higher design pressure values for the ice conditions with larger ice piece mass. For the high level ice concentration, the design pressures based on 2013 and 2014 data differ by approximately 0.35 MPa. In general, the estimated design pressure for the 2014 tests is on average 1.46 times greater than that for the 2013 tests for the ice floe mass ratio of 1.34.

For design pressure estimation, focus is on the tail of the ice load distribution. Here, the analysis was performed considering the top 20% loads of each histogram. A sensitivity analysis was also performed to examine the influence of extreme load sample size used to estimate the design curve parameters ( $\alpha$  and  $x_0$ ) for design pressure estimation, which is presented in Table 7 for 2013 stem loads. There was no significant change of design pressure when derived from different percentages values of extreme loads. However, a sample size, which is too small (e.g., less than the top 10%) or too large (e.g., more than the top 30%) may result in misleading design parameter estimates.

The vessel characteristics, such as structural aspects of the fiberglass hull (e.g., panel stiffness), and panel area, are also factors that influence the ice loads and warrant further investigation. Stiffness of the vessel is a critical consideration for design ice loads as stiffening the structure may increase the resulting ice loads. The interaction time and the deflection of the hull are relatively higher for composite structure vessels than for stiffer steel

**Table 7 Estimated stem local pressures (MPa) considering different percentage of extreme stem loads of 2013 tests**

Transit distance (km)	Stem estimated local pressures (MPa) based on the stem loads of 2013 tests								
	$C_L$ (4–5)			$C_M$ (6–7)			$C_H$ (8–9)		
	10%	20%	30%	10%	20%	30%	10%	20%	30%
0.5	0.48	0.48	0.48	0.60	0.63	0.64	0.68	0.69	0.69
1.0	0.51	0.52	0.51	0.64	0.68	0.69	0.73	0.74	0.74
5.0	0.60	0.60	0.60	0.74	0.79	0.80	0.84	0.84	0.85

structures. For instance, if we consider that a given ice mass dissipates all of its kinetic energy doing work in deflecting a local panel, as illustrated in Fig. 30, we see that a stiff structure will develop higher forces over a shorter distance (and period of time) to absorb the same amount of energy than would be the case for a compliant structure. This is an important consideration for future work, particularly in considering how the results presented in this paper relate to stiffer or larger vessels. Further research is recommended to investigate and quantify these effects in greater detail.

## Conclusions

Full-scale local impact loads measured at two locations on an instrumented TEMPSC were analyzed using the event-maximum method of local pressure estimation to improve understanding of the nature of ice loads for such interactions and to evaluate the suitability of this approach for design load estimation for lifeboats and other GRP vessels in ice. High variability of ice loads has been observed and emphasis in the present work has been placed on the extreme pressures of interest for design. The pressure curve for impact events yielded values of  $\alpha$  and  $x_0$ , parameters that produced conservative design estimates for the conditions considered in this analysis. The effects of the following factors on local pressure estimation have been discussed:

- The mean field ice concentration does not have a clearly defined effect on the magnitude of ice loads; rather these loads depend on the local variation of ice concentration and how the vessel impacted the ice (e.g., straight-line impact). There are more chances for higher peak loads to occur in higher ice concentration due to the increased probability of an impact with two or more ice floes that are packed together. From the data, it was found that most of the high magnitude peak loads occurred at the stem area of the vessel due to straight-line impacts with ice. In addition, the vessel is more exposed in higher ice concentration, which results in a larger number of ice impacts. These are the considerations that lead to the increase of estimated local pressure with increasing ice concentration.
- This method investigated two different ice floe mass cases (similar floe size, but different thickness). Heavier ice floes were observed to transmit significantly higher loads on the vessel.
- The stiffness of the vessel plays a significant role in the magnitude of peak loads measured on the panels. GRP panels are expected to obtain lower peak force than steel structures due to the dissipation of energy over a longer deflection time. This is an important consideration when applying this method for local pressure estimation. This also highlights that the parent distributions for experimental data sets such as these are only representative of the specific structural details and those ice conditions considered in the data sets. Caution must be exercised in applying such data to other, significantly different circumstances. For example, loads estimated for larger, stiffer vessels will likely be under-conservative if these estimates are based on the present data.

The overall distributions of ice loads were also presented in this paper. These operational ice load models provide guidance to the general characteristics of ice loads measured on composite structure vessels operating in certain ice conditions.

The effects of vessel mass, ice floe mass, and vessel speed on the interaction dynamics are complex and not well understood. Additional data including larger and stiffer vessels and larger ice

floes are needed. Further work is also recommended to measure the ice loads on several locations of the vessel having different panel areas to establish a design pressure–area relationship.

## Acknowledgment

The authors would like to thank the Natural Resources Canada's Program of Energy Research and Development (PERD) for financial support that enabled the field program. The first author acknowledges with gratitude the financial support of NSERC (CREATE and Discovery Grants programs). In addition, gratitude is also extended to the National Research Council's trials team for field preparation and logistical support.

## Nomenclature

- $\alpha$  = panel area
- $C, D$  = empirical constants that relate the ice pressure to the nominal contact area
- $C_H$  = high ice concentration
- $C_L$  = low ice concentration
- $C_M$  = medium ice concentration
- $F_Z(z_e)$  = exceedance probability
- $m_{\text{TEMPSC}}$  = TEMPSC mass
- $P_e$  = plotting position
- $r$  = expected proportion of impacts on a given region
- $x$  = random quantity denoting pressure
- $x_0$  = parameter of a pressure curve that represents exposure
- $z_e$  = extreme pressure
- $\alpha$  = parameter that defines the dependence of pressure on contact area
- $v$  = expected number of events

## References

- [1] Kennedy, A., Simões Ré, A., and Veitch, B., 2010, "Operational Limitations of Conventional Lifeboats Operating in Sea Ice," Proceedings of ICETECH, Anchorage, AK, Paper No. ICETECH10-103-RF.
- [2] Bercha, F., 2008, "State of Art of Arctic EER," Proceedings of the 8th International Conference and Exhibition on Performance of Ships and Structures in Ice (ICETECH 2008), Banff, AB, Canada, Paper No. 121-RF.
- [3] International Organization for Standardization (ISO 19906), 2010, *Petroleum and Natural Gas Industries—Arctic Offshore Structures*.
- [4] Jordaan, I. J., Maes, M. A., Browne, P. W., and Hermans, I. P., 1993, "Probabilistic Analysis of Local Ice Pressures," *ASME J. Offshore Mech. Arct. Eng.*, **115**(1), pp. 83–89.
- [5] Taylor, R. S., Jordaan, I. J., Li, C., and Sudom, D., 2010, "Local Design Pressures for Structures in Ice: Analysis of Full-Scale Data," *ASME J. Offshore Mech. Arct. Eng.*, **132**(3), p. 031502.
- [6] Kennedy, A., 2010, "Limitations of Lifeboats Operating in Ice Environments," Master of Engineering thesis, Memorial University of Newfoundland, Faculty of Engineering and Applied Science, St. John's, NL, Canada.
- [7] Simões Ré, A., Veitch, B., Kuczora, A., Barker, A., Sudom, D., and Gifford, P., 2011, "Field Trials of a Lifeboat in Ice and Open Water Conditions," Proceedings of the Port and Ocean Engineering Under Arctic Conditions, Montréal, QC, Canada.
- [8] Simões Ré, A., Veitch, B., Gifford, P., Kennedy, E., Kirby, C., Kuczora, A., and Sudom, D., 2012, "Performance and Survivability of Totally Enclosed Motor Propelled Survival Craft (TEMPSC) in Ice and Open Water Conditions," Ocean, Coastal and River Engineering Portfolio, Paper No. OCRE-TR-2012-07.
- [9] Kennedy, A., Simões Ré, A., and Veitch, B., 2014, "Peak Ice Loads on a Lifeboat in Pack Ice Conditions," Proceedings of the Arctic Technology Conference, Houston, TX.
- [10] Billard, R., Rahman, M. S., Kennedy, A., Simões Ré, A., and Veitch, B., 2014, "Operability of Lifeboats in Pack Ice: Coxswains' Skill and Design Factors," Proceedings of Arctic Technology Conference, Houston, TX, Paper No. OTC 24610.
- [11] Rahman, M. S., Taylor, R. S., Simões Ré, A., Kennedy, A., Wang, J., and Veitch, B., 2014, "Probabilistic Analysis of Local Ice Loads on a Lifeboat," Banff, AB, Canada.